ACS FOOD SCIENCE & TECHNOLOGY

pubs.acs.org/acsfoodscitech

Article

Double Isothermal Amplification and CRISPR-Cas12a for Sensitive Detection of Citrinin

Man Zhang, Xiaoting Xue, Haiyue Gong, Baolin Liu,* and Lei Ye*

Cite This: https://doi.org/10.1021/acsfoodscitech.1c00321

Read Online

ACCESS | Metrics & More | Article Recommendations | Supporting Information

ABSTRACT: An analytical method is developed for ultrasensitive detection of citrinin using double isothermal amplification and CRISPR-Cas12a. Gold nanoparticles (AuNPs) modified with antigen and thiol-terminated, single-strand DNA (ssDNA) are used as a probe. The antigen-modified AuNPs compete with citrinin to bind to magnetic beads coated with an anticitrinin antibody. After a simple magnetic separation, the AuNPs are collected, and the ssDNA are released after they are washed with a dithiothreitol solution. The ssDNA is first amplified by an exponential amplification reaction and then used as a primer in a subsequent hybridization chain reaction to produce double-stranded DNA (dsDNA) that contains a protospacer adjacent motif to allow recognition by CRISPR-Cas12a. The dsDNA activates the Cas12a-gRNA to cleave a reporter ssDNA to generate a fluorescence signal. The developed analytical method has a low detection limit (0.127 ng mL^{-1}) and a wide linear range (0.005−500 μg mL^{-1}) for detection of citrinin. For detection of citrinin in oat and flour, recoveries of 97−104% and 105−111% are obtained, respectively. By combining double isothermal amplification with CRISPR-Cas12a, ultrahigh sensitivity and selectivity can be achieved for detection of toxins in food.

KEYWORDS: *ultrasensitive detection, biobarcode, CRISPR-Cas12a, exponential amplification reaction, hybridization chain reaction, citrinin*

Downloaded via 89.187.185.11 on November 1, 2021 at 10:16:40 (UTC).
See https://pubs.acs.org/sharingguidelines for options on how to legitimately share published articles.

INTRODUCTION

Citrinin (CIT) is a mycotoxin produced by Penicillium, Aspergillus, and Monascus[1] and can be found in corn, wheat, fruits, nuts, and other foods.[2] CIT is nephrotoxic, hepatotoxic, and genotoxic, which makes it a dreadful mycotoxin to humans in spite of its antimicrobial properties.[3] With more attention being paid to food safety, the toxicity of citrinin and the necessity of its detection at low concentration have drawn extensive public attention. Numerous analytical methods have been reported for detection of CIT. For example, high-performance liquid chromatography (HPLC),[4,5] liquid chromatography with tandem mass spectrometry (LC/MS/MS),[6−8] and immunoassays have been developed.[9] These techniques can generate accurate results. However, the complexity of operations, the requirement of skilled personnel, expensive equipment, and time-consuming procedures make them unsuitable for rapid sample analysis. Hence, new detection methods that are rapid, sensitive, and reliable still need to be developed.

Isothermal nucleic acid amplification is able to produce a large number of ssDNA or dsDNA at a constant temperature. Compared with polymerase chain reaction (PCR), it has the advantage that the amplified products can be obtained without changing frequently the reaction temperature.[10−12] This technology is currently widely used in the fields of nucleic acid sequence analysis, genetic engineering, DNA-based materials, and bioimaging.[13−15] The biobarcode assay was proposed by Mirkin[16] and it is now used for molecular detection in a wide range of areas.[17,18] Gao's group has established a series of analytical methods by combining isothermal amplification with biobarcode assays to detect toxins in food. Two recent examples are the detection of T-2 toxin using exponential isothermal amplification (EXPAR)[19] and staphylococcal enterotoxin B using hybridization chain reaction (HCR).[20]

Clustered regularly interspaced short palindromic repeats (CRISPR) and CRISPR-associated proteins (Cas), collectively referred to as CRISPR-Cas, are components of bacterial immune systems.[21,22] CRISPR-Cas12a (Cpf1) proteins are RNA-guided enzymes that bind and cut DNA. Unlike CRISPR-Cas9 proteins, the Cas12a endonucleases only require CRISPR RNA (crRNA) as their guide RNA (g-RNA) to bind a T-rich protospacer-adjacent motif (PAM) to generate dsDNA breaks with staggered 5′ ends.[23,24] To date, CRISPR-Cas12a has been used as a research tool in many areas including genome editing,[25] DNA assembly,[26] and diagnostics.[27,28] The trans cleavage activity of CRISPR-Cas12a on single-strand DNA (ssDNA) has been utilized to detect nucleic acids, and it offers a very useful strategy for improving the specificity, sensitivity, and efficiency of nucleic acid−based diagnosis.[29,30] CRISPR-Cas12a has been combined with loop-mediated amplification (LAMP) to achieve highly sensitive detection of corona virus,[31] hepatitis virus,[32] as

Received: September 3, 2021
Revised: October 8, 2021
Accepted: October 11, 2021

ACS Publications

© XXXX The Authors. Published by American Chemical Society

Scheme 1. Principle of Using Double Isothermal Amplification and CRISPR-Cas12a for Detection of Citrinin

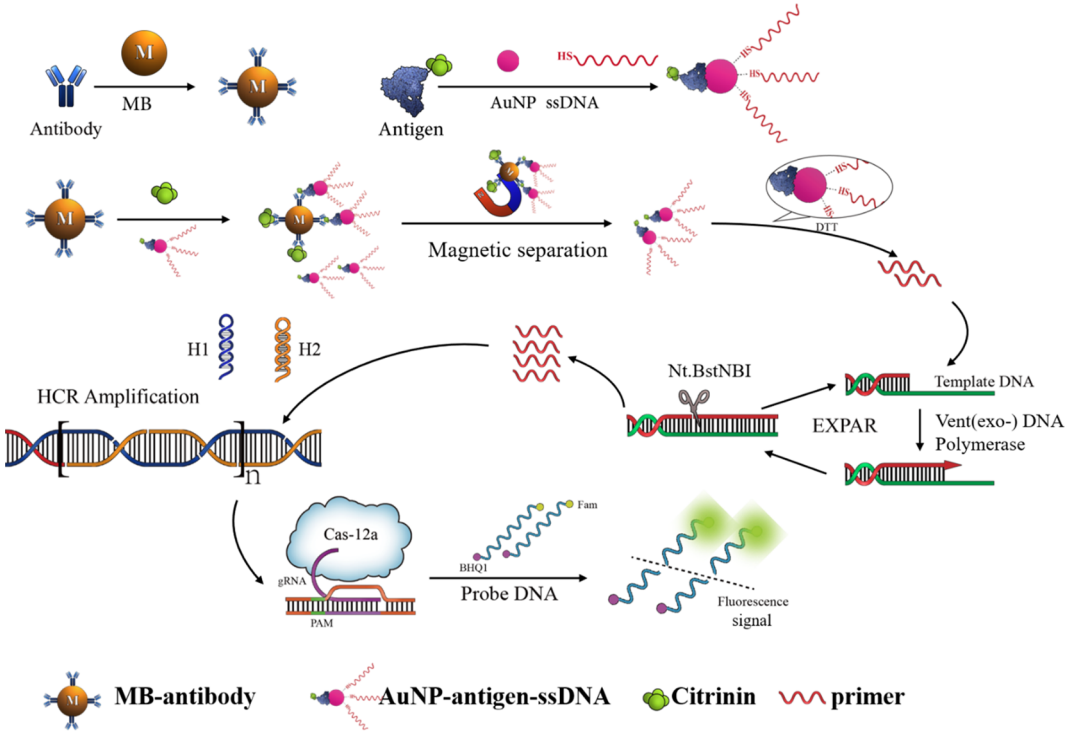


Table 1. DNA Sequences Designed for the Reaction Components Used in This Study

name	sequence (5′−3′)
barcode DNA	SH-AAAAATTAACCTTTCTCCATACGCGGAAGTGAGGT
template	ACCTCACTTCCGCGTATGGAGAAAGGTTAA GAAAGACTCACCTCACTTCCGCGTATGGAGAAAGGTTAA-P
H0	TTAACCTTTCTCCATACGCGGAAG TGAGGT
H1	ACCTCA CTTCCGCGTATGGAGAAAGGTTAA TAAGAC TTAACCTTTCTCCATACGCGGAAG
H2	TTAACCTTTCTCCATACGCGGAAG TGAGGT CTTCCGCGTATGGAGAAAGGTTAA GTCTTA
crRNA	UAAUUUCUACUAAGUGUAGAUUCCAUACGCGGAAGACCUCA
reporter	FAM-GATGCGTACTGTCACTTGAC-BHQ1

well as low-molecular-weight targets.[33] However, combining Cas12a with other isothermal amplification methods to detect small-molecule targets, particularly in the fields of food safety, environmental monitoring, and metabolic engineering has not been explored.

Herein, we establish an analytical method for citrinin detection using biobarcode, double isothermal amplification, and CRISPR-Cas12a to achieve highly sensitive and rapid toxin detection in food. The biobarcode technology is used in a competitive assay format to translate the target binding into a fluorescence signal. The ssDNA on the nanoparticle probe is amplified by EXPAR and HCR to produce a dsDNA that binds and activates Cas12a-gRNA to cleave a ssDNA reporter. With this method, the concentration of CIT can be measured by monitoring the fluorescence intensity after a simple magnetic separation. Using citrinin as a model, one important aim of this work was to demonstrate the general feasibility of double isothermal amplification and CRISPR-Cas12a for analytical detection.

The principle of analyte detection is presented in Scheme 1. In this work, we used a gold nanoparticle labeled with a citrinin antigen as the probe and anticitrinin antibody-coated magnetic beads as the capturing agent. When citrinin is present, there will be a competition between the toxin and the antigen to bind to the antibody. After a magnetic separation, the unbound AuNP probe (AuNP-antigen-ssDNA) can be washed with DTT to release the ssDNA barcode. Therefore, there is a positive relationship between citrinin concentration and the concentration of the released ssDNA barcode. The ssDNA is used as a primer to trigger EXPAR in the presence of a

https://doi.org/10.1021/acsfoodscitech.1c00321
ACS Food Sci. Technol. XXXX, XXX, XXX−XXX

template to replicate efficiently the ssDNA. The ssDNA barcode acts as a primer on the template and is extended by Vent(exo-) DNA polymerase. Since Nt.BstNBI nicking enzyme can cleave single-stranded DNA at a specific site in double-stranded DNA (dsDNA), the primer can be repeatedly extended to obtain a large number of ssDNA barcode (as harpin 0 (H0)). In the HCR step, after addition of the H1 and H2, the ssDNA barcode hybridizes with the H1 to form a double strand H0−H1 structure. Because of the complementary sequences between H1 and H2, strand displacement occurs as soon as the double strand H0−H1 is formed. Therefore, the HCR can generate a large amount of double-stranded DNA (H1−H2) after an initiation by the ssDNA barcode (Figure S1). The dsDNA (H1−H2) is designed to contain the specific, T-rich protospacer-adjacent motif (PAM) for Cas12a. Consequently, Cas12a-gRNA complex can be activated by the amplified dsDNA (H1−H2) to cleave the reporter DNA to generate fluorescence signal.

EXPERIMENTAL SECTION

Reagents and Apparatus. All HPLC-purified oligonucleotide sequences were synthesized by GenScript (Netherlands) and are shown in Table 1. Anticitrinin antibody and citrinin antigen (citrinin-BSA conjugate) were bought from Creative Diagnostics (U.S.A.). Dynabeads Antibody Coupling Kit and Pierce BCA Protein Assay Kit were purchased from Thermo Fisher Scientific Co., Ltd. (U.S.A.). Gold nanoparticles (15 nm, stabilized suspension in 0.1 mM PBS, ∼1.64 × 10^{12} particles mL^{-1}) were purchased from Sigma-Aldrich (Sweden). EnGen Lba Cas12a (Cpf1), Nt.BstNBI nicking enzyme, Vent(exo-) DNA polymerase, NEBuffer 3.1 and dNTPs were obtained from New England BioLabs (Ipswich, MA, U.S.A.). Citrinin (CIT), Zearalenone (ZEN), Fumonisin B1 (FB1) and Ochratoxin A (OTA) were obtained from AH Diagnostics AB (Sweden). All the other chemicals (analytical reagent) were obtained from commercial sources and were used without additional purification. All buffers were prepared with purified water from a Milli-Q water purification system (Millipore Corp., Bedford, U.S.A.). Fluorescence measurements were performed with Cary Eclipse Fluorescence Spectrophotometer (Agilent Technologies, Germany). Zeta potential was measured with a dynamic light scattering instrument (Malvern Panalytical, Spectris Company, U.K.). UV−vis spectrometry was carried out using a Cary 60 UV−vis spectrophotometer (Agilent Technologies, U.S.A.).

Immobilization of Anticitrinin Antibody on Magnetic Beads (MBs). Anticitrinin antibody was immobilized on magnetic beads (Dynabeads M-270 Epoxy beads) using a coupling kit provided by Thermo Fisher Scientific. BCA protein assay kit was used to determine the coupling efficiency. The final concentration of the antibody-coated MBs was ∼1 mg mL^{-1}.

Preparation of AuNP-Antigen-DNA Probe. AuNP-antigen-DNA probe was prepared using a previously published method.[34] The antigen was adsorbed on the surface of the gold nanoparticles through electrostatic interaction, and the ssDNA was conjugated via the sulfhydryl group to the AuNPs. In the first step, colloidal gold solution (1 mL) was mixed with 0.1 M Na_2CO_3 solution (20−25 μL) to adjust the pH to 8.5−9.0. Then, 100 μL of citrinin antigen (220 μg mL^{-1} in water) was added to the colloidal gold solution and shaken for 1 h at room temperature. In the second step, 100 μL of the ssDNA (10 μM in water) was added into the mixture and incubated at 4 °C for 2 h. Next, 110 μL of 10% PEG 20000 and 130 μL of salting buffer (1.4 M NaCl, 0.1 M PBS) were added, and the mixture was incubated at room temperature for 2 h. In the last step, 50 μL of freshly prepared 5% BSA was added, and the mixture was incubated at 4 °C for 1 h. The mixture was centrifuged at 13 000 rpm for 20 min at 4 °C. After removing the supernatant, 1 mL of washing solution (1% PEG 20000, 1% BSA, 0.1 M PBS) was added to disperse the nanoparticles. The obtained mixture was gently stirred at 4 °C for 1 h. After a final centrifugation, the AuNP-antigen-DNA probe was resuspended in 500 μL of washing solution and stored at 4 °C until use.

Competitive Assay Based on Biobarcode. Citrinin solution was diluted to 0.005, 0.05, 0.5, 5, 50, and 500 μg mL^{-1} in 10% (v/v) DMSO/PBS. The citrinin solution (50 μL) was mixed with 20 μL of the AuNP-antigen-DNA probe solution and 20 μL of the antibody-coated MBs. The mixture was shaken at 37 °C for 1 h. During this period, citrinin competed with the AuNP-antigen-DNA probe to bind to the antibody immobilized on the MBs. The resulting solution was left on a magnet for 3 min to separate the MBs. The supernatant was collected and shaken with 100 μL of 5 mM DTT at 25 °C for 60 min to release the barcode DNA. After the sample was centrifuged at 6000 rpm for 10 min, the supernatant containing the ssDNA was collected for use in the next amplification step.

Exponential Amplification Reaction (EXPAR) and Hybridization Chain Reaction (HCR). The isothermal amplification was divided into two parts. In Part I of the EXPAR, 10 μL of template DNA (1 μM) and 10 μL of the ssDNA barcode (as primer) were mixed in 5 μL of 10× NEB buffer 3.1 (the 1× buffer contains 100 mM NaCl, 50 mM Tris-HCl, 10 mM $MgCl_2$, 100 μg mL^{-1} BSA, pH 7.9). The mixture was incubated at 95 °C for 5 min and then gradually cooled to room temperature. Then, 2 μL of Nt.BstNBI nicking enzyme (4 U/μL), 3 μL of Vent(exo-) DNA polymerase (1 U/μL), 5 μL of 10× ThermoPol buffer (the 1× buffer contains 10 mM $NaNO_3$, 20 mM Tris-HNO_3, 2 mM $Mg(NO_3)_2$, 0.1% Triton X-100, pH 8.8), and 10 μL of 10 mM dNTPs were added. The total reaction volume was adjusted to 50 μL with water. The mixture was incubated at 55 °C for 50 min and then stored at 4 °C. In Part II of the HCR, 10 μL of 10 μM hairpin DNA 1 (H1) and 10 μL of 10 μM hairpin DNA 2 (H2) were first mixed and incubated at 95 °C for 5 min and then slowly cooled to room temperature. The 20 μL obtained solution (H1+H2) and 170 μL of hybridization buffer (Tris 50 mM, NaCl 400 mM, $MgCl_2$ 5 mM, pH 7.4) were added into the 10 μL reaction product from Part I to make a final reaction volume of 200 μL. The final mixture was incubated at 37 °C for 60 min before it was stored at 4 °C for the next step.

Gel Electrophoresis. Gel electrophoresis was performed to verify the EXPAR and HCR products. The 12% native polyacrylamide gel was prepared with 3 mL of 5× TBE buffer (1× buffer contains 90 mM Tris-HCl, 2 mM EDTA, 90 mM boric acid, pH 7.8), 6 mL of water, 6 mL of 30% acrylamide/bis-acrylamide (29/1), 10 μL of TEMED, and 110 μL of 10% freshly prepared ammonium persulfate (APS). The electrophoresis was run at 275−300 V for 1 h in 0.5× TBE buffer. The gel was stained with Gel-green for 40 min and visualized using a Bio-Rad gel imager.

Preparation of Cas12a-gRNA Complex and LbCas12a Trans-Cleavage. LbCas12a (cpf1) (500 nM, 10 μL) was incubated with 12.5 μL of 500 nM gRNA in 77.5 μL of 1× NEB buffer 2.1 for 30 min at 37 °C to form the RNA-protein complex. The final concentrations of LbCas12a and crRNA in the solution were 50 nM and 62.5 nM, respectively. After addition of 5 μL of the reporter DNA (1 μM), 20 μL of the amplification products, and 75 μL of 1× NEB buffer 2.1, the mixture was shaken and incubated at 37 °C for 30 min. During this period, the dsDNA activated the Cas12a-gRNA to cut the ssDNA reporter to generate fluorescence signal. The excitation wavelength was set to 488 nm, and the emission wavelength of the fluorescence peak was 520 nm.

Detection of Citrinin in Oat and Flour. Oat and flour were purchased from a local supermarket in Lund. The method of sample preparation was adopted from a previous work by Mandal et al.[35] Powdered flour and oat samples (1 g) were spiked with 100 μL of citrinin solution (0.1 μg mL^{-1}, 1 μg mL^{-1}, 10 μg mL^{-1}) prepared in 10% acetonitrile in water. The spiked samples were extracted with 10 mL of 70% methanol by ultrasonication (15 min) and centrifugation at 2000 rpm for 10 min, following protocols mentioned by the European Food Safety Authority.[36] The supernatant (1 mL) was evaporated to dryness, and the residue was redissolved in 100 μL of 10% acetonitrile in water. The obtained solution (50 μL) was then used in the competitive assay based on DNA barcode and isothermal amplification (as described in the sections Competitive Assay Based on Biobarcode and Preparation of Cas12a-gRNA Complex and LbCas12a Trans-Cleavage) to measure the citrinin concentration.

https://doi.org/10.1021/acsfoodscitech.1c00321
ACS Food Sci. Technol. XXXX, XXX, XXX−XXX

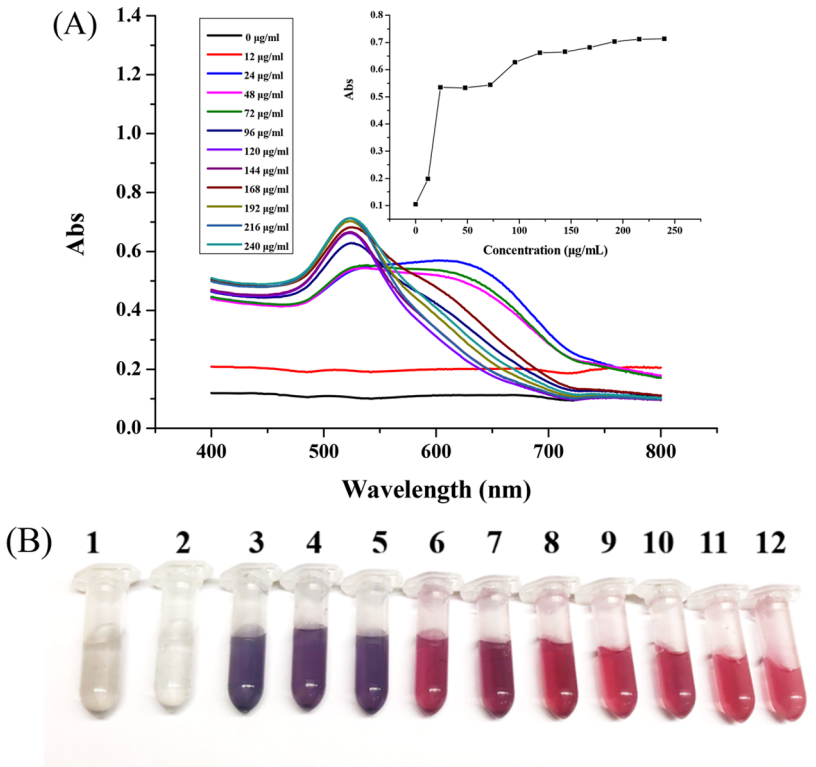


Figure 1. (A) UV−vis absorption spectra of AuNPs after incubation with different concentrations of antigen (0−240 μg mL^{-1}). The inset shows the absorbance measured at 525 nm. (B) Visual color changes caused by different antigen concentration corresponding to (A).

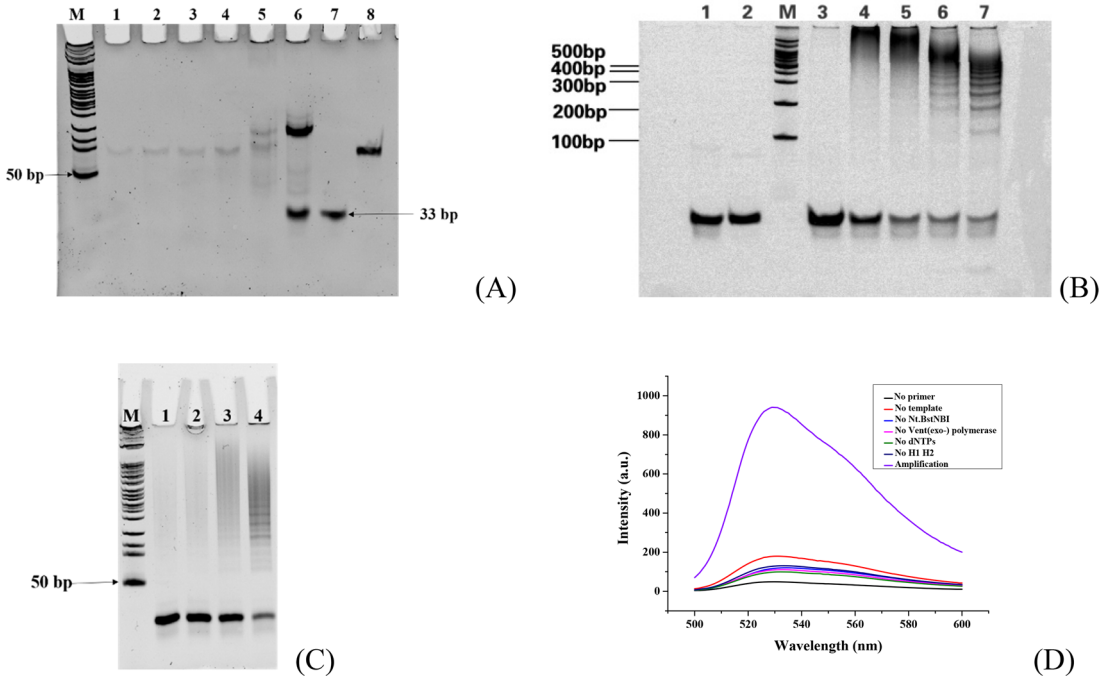


Figure 2. (A) Gel electrophoresis of DNA products amplified by EXPAR using different concentrations of primer. The lanes from left to right are M: 50 bp marker; lane 1: primer 0 nM; lane 2: primer 1 nM; lane 3: primer 10 nM; lane 4: primer 100 nM; lane 5: primer 1 μM ; lane 6: primer 10 μM; lane 7: only primer (10 μM); lane 8: only template (10 μM). (B) Gel electrophoresis of DNA products amplified by HCR. The lanes from left to right are lane 1: H1 (10 μM); lane 2: H2 (10 μM); M: 500 bp marker; lane 3: H1+H2 (10 μM), H0 (0 μM); lane 4: H1+H2 (10 μM), H0: (5 pM); lane 5: H1+H2 (10 μM), H0 (10 pM); lane 6: H1+H2 (10 μM), H0 (20 pM); lane 7: H1+H2 (10 μM), H0 (40 pM). (C) Gel electrophoresis of DNA products amplified by EXPAR and HCR. M: 50 bp marker; lane 1: primer 0 μM (template 10 μM, H1+H2 10 μM); lane 2: primer 10 pM (template 10 μM, H1+H2 10 μM); lane 3: primer 20 pM (template 10 μM, H1+H2 10 μM); lane 4: primer 40 pM (template 10 μM, H1+H2 10 μM). All the concentrations mentioned are values of the stock reagent solutions. (D) Fluorescence spectra of products from the double amplification reactions where none or one of the reaction components is not present. Excitation/emission wavelength: 488 nm/520 nm.

https://doi.org/10.1021/acsfoodscitech.1c00321
ACS Food Sci. Technol. XXXX, XXX, XXX−XXX

RESULTS AND DISCUSSION

Characterization of MBs and AuNP Probe. In order to find out the most suitable concentration of antigen to be immobilized on the gold nanoparticles, we used UV spectrophotometer to monitor the antigen binding to the AuNPs. As shown in Figure 1A, a series of antigen solution of different concentration (0−240 μg mL^{-1}) were first added to the AuNPs in pH 9 buffer. Then, 100 μL of 1 M NaCl solution was added, and the mixture was kept at room temperature for 2 h. Because of the addition of the salt solution, AuNPs tend to aggregate if the nanoparticles were not coated and protected by the protein, causing the color of the solution to turn to gray, as seen in Figure 1B. Above the optimal concentration of antigen, the color of the antigen-coated AuNPs did not change. Based on the UV spectrum of the antigen-treated AuNPs, the optimal antigen concentration was determined to be 192 to 240 μg mL^{-1}. Above this concentration, the absorption peak did not shift, and the color did not change appreciably. Accordingly, the optimal concentration of the antigen was 220 μg mL^{-1}.

We used Zeta potential and UV spectra to characterize the gold nanoparticles before and after modification with the antigen. As shown in Figure S2, AuNPs, AuNP-antigen and AuNP-antigen-DNA had a Zeta potential of −13.88, −19.95, and −30.11 mV, respectively. The value of the Zeta potential was related to the stability of the colloidal dispersion. A large negative Zeta potential indicates a dense coverage of negatively charged molecules on the AuNPs, confirming successful preparation of AuNP-antigen-ssDNA probe.[37] In the UV spectra, the unmodified AuNPs had a strong absorption peak at 515 nm (Figure S3). For the AuNP-antigen-DNA probe, the peak shifted to 525 nm (10 nm redshift) and became significantly weaker. The reason for the red shift was the change of particle size and interparticle distance.[38] The decrease in absorbance was due to the loss of the nanoparticles during the multiple centrifugation and washing steps.

The amount of antibody immobilized on the MBs was calculated from the unbound fraction measured using a BCA protein quantification kit (Figure S4). The antibody coupling efficiency on the surface of the MBs was calculated as 84.7%, which confirmed successful immobilization of antibody on the MBs.

Feasibility Verification and Optimization of Assay Conditions. In order to explore the feasibility of the analytical procedure, we first verified the nucleic acid amplification by EXPAR. The amplification products were analyzed through gel electrophoresis. In Figure 2A, lanes 1 to 6 were the amplification products obtained using different concentrations of the primer, lanes 7 and 8 were the primer and the template DNA, respectively. It can be seen that as the primer concentration increased to 10 μM, the intensity of the amplified ssDNA band (33 bp) became obvious, which indicated that the amplification by EXPAR proceeded smoothly. Additional EXPAR experiments were carried out by varying the concentration of the primer from 1 to 10 μM. As shown in Figure S5, with a primer concentration of 5 μM, the amplified ssDNA band became visible in the electrophoresis gel. When the system was lacking any essential component (e.g., the enzymes or dNTPs), the ssDNA band did not appear even at a concentration of 10 μM (Figure S6). To explore the feasibility of HCR amplification, the reaction products were also analyzed using gel electrophoresis (Figure 2B). Lanes 1 and 2 represent the H1 and H2, respectively. Lanes 3 to 7 were the amplified products generated after addition of H0 at varying concentrations. It can be clearly seen that when H0 was absent, the hairpin cannot be opened, and H1 and H2 alone were not able to spontaneously produce hybridized products. Upon addition of a small amount of H0, the amplified product with a larger bp number started to appear. With the concentration of H0 increased, more dsDNA products with a lower bp number were formed, and the electrophoretic bands became more intense. This result proved that the designed DNA sequences worked well in the HCR. Finally, we combined the EXPAR and HCR to verify the double nucleic acid amplifications by analyzing the products using gel electrophoresis (Figure 2C). In this experiment, the EXPAR products initiated by the ssDNA primer acted as H0, which triggered H1 and H2 to form dsDNA products. In Figure 2C, it can be seen that the more primer added, the more products were obtained in the EXPAR amplification, which caused more hairpin DNA to be opened in the HCR resulting in more dsDNA products.

In order to further prove the successful double isothermal amplification, the product of EXPAR and HCR was added to Cas12a-gRNA and the ssDNA reporter to observe the emitted fluorescence signal. As seen in Figure 2D, when any component of the amplification system was missing, it was not possible to achieve effective amplification, and the fluorescence signals were very weak. Without the EXPAR reaction (caused by omission of the template, the nicking enzyme, the polymerase, or the dNTPs), the HCR reaction alone was not able to generate enough activated Cas12a to produce strong fluorescence emission. Only when all essential components for the dual amplification were present, the ssDNA primer was able to initiate effective nucleic acid amplification to activate the Cas12a-gRNA to produce the fluorescence. The importance of the EXPAR was further confirmed by studying the fluorescence output generated by HCR in a separate experiment. As shown in Figure S7, although the HCR products generated by different concentrations of H0 (up to 100 nM) was able to activate the Cas12a-gRNA to generate the fluorescence signal, the intensity of the signal was much lower than that was obtained by the dual amplification (Figure 2D).

During our preliminary experiments to verify the amplification and Cas12a-catalized reactions, we observed that the concentrations of Vent(exo-) DNA polymerase, Nt.BstNBI enzyme and the hairpin DNA H1 and H2 had a great influence on the test results. Therefore, these parameters were optimized to establish a suitable fluorescence detection system. As shown in Figure S8, the fluorescence increased steadily with the concentration of Vent(exo-) DNA polymerase until an optimal enzyme loading, then the fluorescence change became gradual when more enzyme was used. The optimum amount of Vent(exo-) DNA polymerase was 1 U μL^{-1}. For Nt.BstNBI, the fluorescence signal also increased with the enzyme concentration. The optimal concentration was found to be 4 U μL^{-1}. Similarly, because of the significant role of H1 and H2 in the overall amplification, we also studied the optimal concentration of H1 and H2, and we obtained the best results with 10 μM of the hairpin DNA. For the Cas12a-gRNA reaction, the incubation time and temperature were optimized by monitoring the final fluorescence emission (Figure S9). To study the temperature effect, we used two different concentrations of amplification products as activators to

https://doi.org/10.1021/acsfoodscitech.1c00321
ACS Food Sci. Technol. XXXX, XXX, XXX−XXX

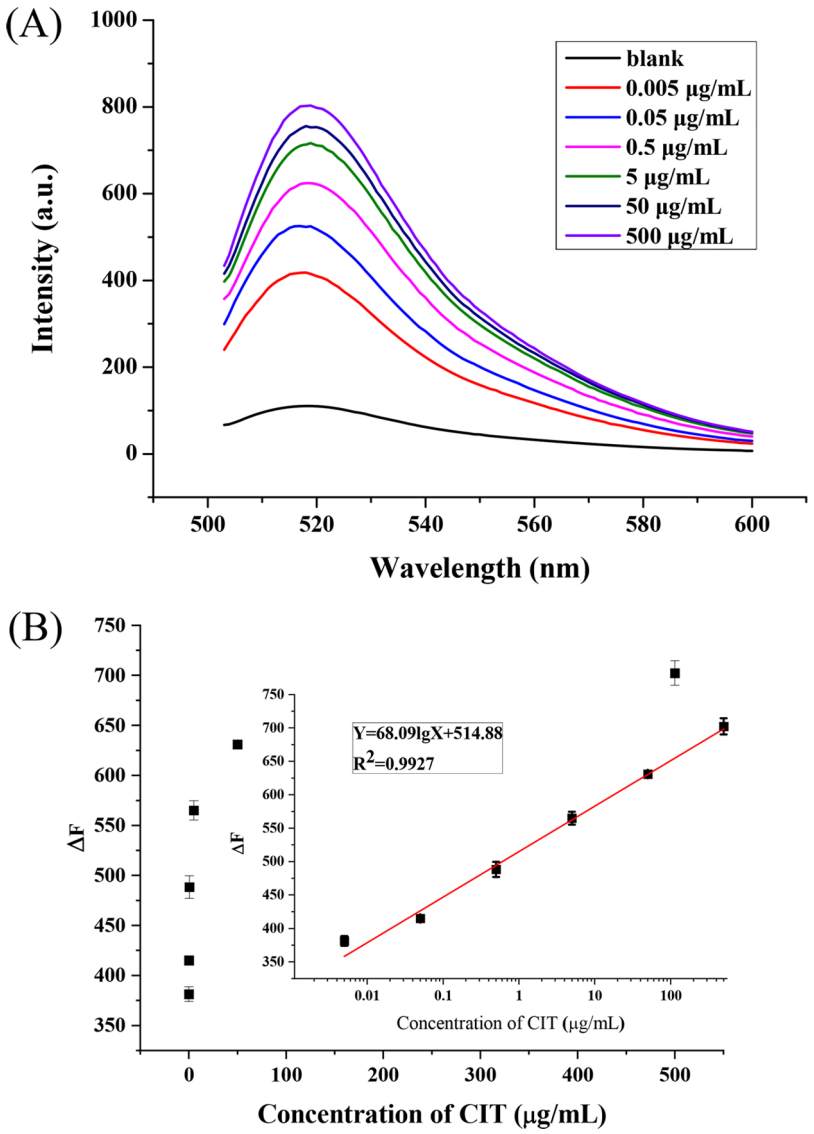


Figure 3. (A) Fluorescence spectra of assayed samples containing different concentrations of CIT (0.005−500 μg mL^{-1}). (B) Relationship between CIT concentration and fluorescence intensity. For CIT concentration in the range of 0.005−500 μg mL^{-1}, the linear equation is y = 68.09 lg(x) + 514.88 (with R^2 = 0.9927).

Table 2. Comparison of Analytical Methods for Detection of CIT

methods	linear range	LOD	sample	ref
MIP electrochemical sensor	1.0 × 10^{-12}−1.0 × 10^{-10} M	2.0 × 10^{-13} M	rye sample	39
FRET-based immunosensor	1 × 10^{-12}−6 × 10^{-12} M	1 × 10^{-13} M	human serum	40
LC-MS/MS	0.1−100 μg L^{-1}	1.0 μg kg^{-1}	fermented rice	41
QDs with MIP	1.0 × 10^{-9}−5.0 × 10^{-9} M	2.0 × 10^{-10} M	chicken egg	42
electro-capillary/CG	0.08−10 μg mL^{-1}	0.03 μg mL^{-1}	red yeast rice	43
spectrofluorimetric	0−0.15 μg mL^{-1}	1.0 μg kg^{-1}	rice	44
ELISA/AuNPs strip	28.6−9454 ng g^{-1}	20 ng mL^{-1}	fermented food	45
hybrid MIP membranes	5−100 ng g^{-1}	0.5 ng g^{-1}	rice	46
Cas12a/EXPAR-HCR	0.005−500 μg mL^{-1}	0.127 ng mL^{-1}	oat and flour	this work

measure the fluorescence emission at 25 °C, 30 °C, and 37 °C. On the basis of the fluorescence intensity, the best incubation temperature was determined to be 37 °C for the two activator concentrations. Figure S9B shows that when the incubation time was longer than 30 min, the fluorescence intensity did not increase further. Therefore, 30 min was chosen as the optimal time for the Cas12a-gRNA reaction.

Fluorescence Assay for Citrinin. Using the above optimized conditions, a series of citrinin solutions at different concentrations were measured with the fluorescence assay. Citrinin at the different concentrations (0, 0.005, 0.05, 0.5, 5, 50, 500 μg mL^{-1}) competed with the AuNP-antigen-DNA probe for binding to the antibody-coated MBs. The unbound AuNP-antigen-DNA probe was collected to release the ssDNA

https://doi.org/10.1021/acsfoodscitech.1c00321
ACS Food Sci. Technol. XXXX, XXX, XXX−XXX

for the EXPAR and HCR amplification. The concentration of unbound DNA after the magnetic separation can be quantified by UV spectrometry. In Figure S10, when the concentration of citrinin was increased, the concentration of the unbound DNA also became higher. Figure 3A shows the change of fluorescence intensity of the samples caused by citrinin at the different concentrations. The correlation between citrinin concentration and the fluorescence intensity is clearly seen in Figure 3B. This semilogarithmic plot exhibits a linear relationship between the fluorescence intensity and the logarithm of citrinin concentration in the range of 0.005−500 μg mL^{-1}, with a detection limit of 0.127 ng mL^{-1} (S/N = 3). In Table 2, we provide a comparison of the analytical performance of our fluorescence assay with some previously reported methods. The very low limit of detection and the simple fluorescence readout are of particular advantages for detection of toxins in food.

Specificity of Fluorescence Assay for Citrinin. To evaluate the specificity of the fluorescence assay, we studied the signal responses caused by citrinin and its structural analogues under the same assay conditions. For this experiment, the ssDNA, H0, and the template DNA were ordered from Sangon Biotech (Shanghai, China). As shown in Figure 4, the

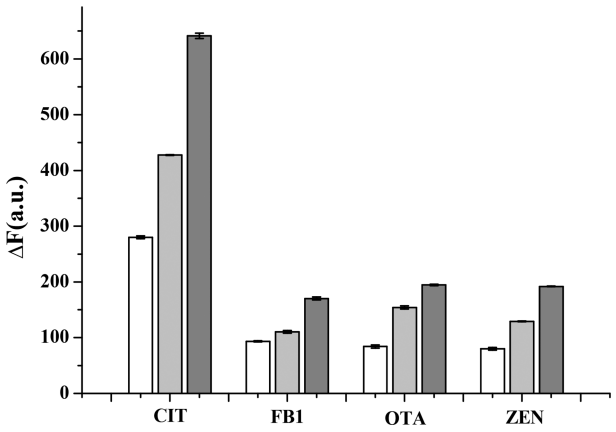


Figure 4. Evaluation of specificity of the fluorescence assay. The signal intensity generated from CIT is compared with that from ZEN, OTA, and FB1 at three different concentrations (from left to right) of 1, 10, and 1000 ng mL^{-1}.

fluorescence signals caused by FB1, ZEN, and OTA were very weak, as these citrinin analogues were not able to bind the anticitrinin antibody on the MBs to displace the AuNP-antigen-DNA probe. Collectively, by combining double isothermal amplification with CRISPR-Cas12a, the competitive fluorescence assay offers a convenient method to detect citrinin with a very high selectivity.

Detection of Citrinin in Real Samples. The accuracy of the assay was assessed by the recovery of citrinin in spiked oat and flour samples. A citrinin solution was added to oat and flour samples purchased from a local supermarket. As shown in Table 3, the average recoveries of citrinin from the spiked oat and flour samples were 96.7−104% and 105−111%, respectively. The relative standard deviations (RSDs) were 5.29−10.3% and 4.76−9.16% for the oat and flour samples, respectively. These results confirm that the double isothermal amplification and CRISPR-Cas12a reaction, the two critical components to enable high selectivity and sensitivity in the fluorescence assay, are fully compatible with complex food

Table 3. Recovery of CIT at Different Concentration Levels in Oat and Flour (n = 6)

		results using Cas12a-gRNA with EXPAR and HCR	
sample	spiked concentration (μg mL^{-1})	recovery (%)	RSD (%)
oat	0.1	96.7	6.33
	1	104	10.3
	10	97.3	5.29
flour	0.1	111	9.16
	1	105	4.76
	10	106	5.48

samples. The duration of the entire workflow was 2.5 h, including sample preparation (10 min), EXPAR (50 min), HCR (60 min), and CRISPR/Cas12a reaction (30 min).

By combining biobarcode technology with a two-step isothermal nucleic acid amplification (EXPAR and HCR) and Cas12a-gRNA reaction, we have developed a competitive fluorescence assay for a food toxin citrinin. The use of CRISPR-Cas12a to generate the optical signal and the biobarcode and double isothermal amplification have led to ultrasensitive detection of citrinin with a limit of detection (0.127 ng mL^{-1}) much lower than traditional methods. The tandem EXPAR and HCR offers more efficient amplification of the analytical response. The use of Cas12a-gRNA allows fluorescence signal to be generated in real time without tedious separation steps. Moreover, this is the first report of detecting small toxins in food by combining double isothermal amplification with CRISPR-Cas12a technology. The assay is easy to carry out and does not require expensive equipment. One disadvantage is the relatively high cost of reagents compared with traditional ELISA, for example. With further development and improvement, the demonstrated principle of analysis will bring in a series of easy-to-use analytical tools to improve food safety, environmental monitoring, and medical diagnostics.

■ ASSOCIATED CONTENT

Supporting Information

The Supporting Information is available free of charge at https://pubs.acs.org/doi/10.1021/acsfoodscitech.1c00321.

Additional experimental data of Zeta potential, UV−vis spectra, protein assay, gel electrophoresis, and fluorescence measurement (PDF)

■ AUTHOR INFORMATION

Corresponding Authors

Baolin Liu − *School of Medical Instrument and Food Engineering, University of Shanghai for Science and Technology, Shanghai 200093, China*; Email: blliuk@163.com

Lei Ye − *Division of Pure and Applied Biochemistry, Department of Chemistry, Lund University, 22100 Lund, Sweden*; orcid.org/0000-0002-3646-4072; Email: lei.ye@tbiokem.lth.se

Authors

Man Zhang − *Division of Pure and Applied Biochemistry, Department of Chemistry, Lund University, 22100 Lund, Sweden; School of Medical Instrument and Food Engineering, University of Shanghai for Science and Technology, Shanghai 200093, China*

https://doi.org/10.1021/acsfoodscitech.1c00321
ACS Food Sci. Technol. XXXX, XXX, XXX−XXX

Xiaoting Xue − *Division of Pure and Applied Biochemistry, Department of Chemistry, Lund University, 22100 Lund, Sweden;* orcid.org/0000-0002-3716-3132

Haiyue Gong − *Division of Pure and Applied Biochemistry, Department of Chemistry, Lund University, 22100 Lund, Sweden;* orcid.org/0000-0002-9357-7364

Complete contact information is available at: https://pubs.acs.org/10.1021/acsfoodscitech.1c00321

Author Contributions

M.Z.: Methodology, investigation, data curation, writing - original draft. X.X.: Material characterization, discussion of results. H.G.: Material characterization, discussion of results. B.L.: Supervision, project administration. L.Y.: Supervision, project administration, writing - review and editing, funding acquisition.

Funding

This research was funded by the Swedish Research Council VR (grant number 2019-04228) and FORMAS (grant number 2016-00591) and the China Scholarship Council (award number 201908310065).

Notes

The authors declare no competing financial interest.

■ ACKNOWLEDGMENTS

We thank the Swedish Research Council VR and FORMAS for financial support to this project. M.Z. thanks the China Scholarship Council for supporting her visit to Lund University.

■ REFERENCES

(1) Xu, B.-J.; Jia, X.-Q.; Gu, L.-J.; Sung, C.-K. Review on the qualitative and quantitative analysis of the mycotoxin citrinin. *Food Control* **2006**, *17*, 271−285.

(2) Ostry, V.; Malir, F.; Ruprich, J. Producers and important dietary sources of ochratoxin A and citrinin. *Toxins* **2013**, *5*, 1574−1586.

(3) Doughari, J. H. The occurrence, properties and significance of citrinin mycotoxin. *J. Plant Pathol. Microbiol.* **2015**, *6*, 321.

(4) Huertas-Pérez, J. F.; Arroyo-Manzanares, N.; García-Campaña, A. M.; Gámiz-Gracia, L. High-throughput determination of citrinin in rice by ultra-high-performance liquid chromatography and fluorescence detection (UHPLC-FL). *Food Addit. Contam., Part A* **2015**, *32*, 1352−1357.

(5) Vazquez, B.; Fente, C.; Franco, C.; Cepeda, A.; Prognon, P.; Mahuzier, G. Simultaneous high-performance liquid chromatographic determination of ochratoxin A and citrinin in cheese by time-resolved luminescence using terbium. *J. Chromatogr. A* **1996**, *727*, 185−193.

(6) Shu, P.-Y.; Lin, C.-H. Simple and sensitive determination of citrinin in Monascus by GC-selected ion monitoring mass spectrometry. *Anal. Sci.* **2002**, *18*, 283−287.

(7) Lee, C.-L.; Wang, J.-J.; Pan, T.-M. Synchronous analysis method for detection of citrinin and the lactone and acid forms of Monacolin K in red mold rice. *J. AOAC Int.* **2006**, *89*, 669−677.

(8) Odhav, B.; Naicker, V. Mycotoxins in south african traditionally brewed beers. *Food Addit. Contam.* **2002**, *19*, 55−61.

(9) Xu, Y.; Ma, B.; Chen, E.; Yu, X.; Ye, Z.; Sun, C.; Zhang, M. Dual fluorescent immunochromatographic assay for simultaneous quantitative detection of citrinin and zearalenone in corn samples. *Food Chem.* **2021**, *336*, 127713.

(10) Zeng, R.; Luo, Z.; Su, L.; Zhang, L.; Tang, D.; Niessner, R.; Knopp, D. Palindromic molecular beacon based Z-scheme BiOCl-Au-CdS photoelectrochemical biodetection. *Anal. Chem.* **2019**, *91*, 2447−2454.

(11) Zhang, K.; Lv, S.; Lin, Z.; Li, M.; Tang, D. Bio-barcode-based photoelectrochemical immunoassay for sensitive detection of prostate-specific antigen using rolling circle amplification and enzymatic biocatalytic precipitation. *Biosens. Bioelectron.* **2018**, *101*, 159−166.

(12) Zhang, K.; Lv, S.; Lin, Z.; Tang, D. CdS:Mn quantum dot-functionalized g-C_3N_4 nanohybrids as signal-generation tags for photoelectrochemical immunoassay of prostate specific antigen coupling DNAzyme concatamer with enzymatic biocatalytic precipitation. *Biosens. Bioelectron.* **2017**, *95*, 34−40.

(13) Xia, H.; Li, L.; Yin, Z.; Hou, X.; Zhu, J.-J. Biobar-coded gold nanoparticles and DNAzyme-based dual signal amplification strategy for ultrasensitive detection of protein by electrochemiluminescence. *ACS Appl. Mater. Interfaces* **2015**, *7*, 696−703.

(14) Liu, S.; Wang, Y.; Ming, J.; Lin, Y.; Cheng, C.; Li, F. Enzyme-free and ultrasensitive electrochemical detection of nucleic acids by target catalyzed hairpin assembly followed with hybridization chain reaction. *Biosens. Bioelectron.* **2013**, *49*, 472−477.

(15) Song, S.; Fan, C. RCA-assisted self-assembled DNA origami nano-constructs as vehicles for cellular delivery of diagnostic probes and therapeutic drugs. *Rolling Circle Amplification (RCA)*; Springer, 2016; pp 151−159.

(16) Thaxton, C. S.; Elghanian, R.; Thomas, A. D.; Stoeva, S. I.; Lee, J.-S.; Smith, N. D.; Schaeffer, A. J.; Klocker, H.; Horninger, W.; Bartsch, G.; Mirkin, C. A. Nanoparticle-based bio-barcode assay redefines "undetectable" PSA and biochemical recurrence after radical prostatectomy. *Proc. Natl. Acad. Sci. U. S. A.* **2009**, *106*, 18437−18442.

(17) Amini, B.; Kamali, M.; Salouti, M.; Yaghmaei, P. Fluorescence bio-barcode DNA assay based on gold and magnetic nanoparticles for detection of Exotoxin A gene sequence. *Biosens. Bioelectron.* **2017**, *92*, 679−686.

(18) Choi, H. M.; Beck, V. A.; Pierce, N. A. Next-generation in situ hybridization chain reaction: higher gain, lower cost, greater durability. *ACS Nano* **2014**, *8*, 4284−4294.

(19) Zhang, M.; Wang, Y.; Yuan, S.; Sun, X.; Huo, B.; Bai, J.; Peng, Y.; Ning, B.; Liu, B.; Gao, Z. Competitive fluorometric assay for the food toxin T-2 by using DNA-modified silver nanoclusters, aptamer-modified magnetic beads, and exponential isothermal amplification. *Microchim. Acta* **2019**, *186*, 1−7.

(20) Xu, Y.; Huo, B.; Sun, X.; Ning, B.; Peng, Y.; Bai, J.; Gao, Z. Rapid detection of staphylococcal enterotoxin B in milk samples based on fluorescence hybridization chain reaction amplification. *RSC Adv.* **2018**, *8*, 16024−16031.

(21) Zetsche, B.; Gootenberg, J. S.; Abudayyeh, O. O.; Slaymaker, I. M.; Makarova, K. S.; Essletzbichler, P.; Volz, S. E.; Joung, J.; Van Der Oost, J.; Regev, A.; et al. Cpf1 is a single RNA-guided endonuclease of a class 2 CRISPR-Cas system. *Cell* **2015**, *163*, 759−771.

(22) Schunder, E.; Rydzewski, K.; Grunow, R.; Heuner, K. First indication for a functional CRISPR/Cas system in Francisella tularensis. *Int. J. Med. Microbiol.* **2013**, *303*, 51−60.

(23) Gong, H.; Wu, Y.; Zeng, R.; Zeng, Y.; Liu, X.; Tang, D. CRISPR/Cas12a-mediated liposome-amplified strategy for the photoelectrochemical detection of nucleic acid. *Chem. Commun.* **2021**, *57*, 8977−8980.

(24) Zeng, R.; Wang, W.; Chen, M.; Wan, Q.; Wang, C.; Knopp, D.; Tang, D. CRISPR-Cas12a-driven MXene-PEDOT: PSS piezoresistive wireless biosensor. *Nano Energy* **2021**, *82*, 105711.

(25) Jiang, Y.; Qian, F.; Yang, J.; Liu, Y.; Dong, F.; Xu, C.; Sun, B.; Chen, B.; Xu, X.; Li, Y.; et al. CRISPR-Cpf1 assisted genome editing of Corynebacterium glutamicum. *Nat. Commun.* **2017**, *8*, 1−11.

(26) Lei, C.; Li, S.-Y.; Liu, J.-K.; Zheng, X.; Zhao, G.-P.; Wang, J. The CCTL (Cpf1-assisted Cutting and Taq DNA ligase-assisted Ligation) method for efficient editing of large DNA constructs in vitro. *Nucleic Acids Res.* **2017**, *45*, e74.

(27) Zuo, X.; Fan, C.; Chen, H.-Y. Biosensing: CRISPR-powered diagnostics. *Nat. Biomed. Eng.* **2017**, *1*, 0091.

(28) Chertow, D. S. Next-generation diagnostics with CRISPR. *Science* **2018**, *360*, 381−382.

(29) Chen, J. S.; Ma, E.; Harrington, L. B.; Da Costa, M.; Tian, X.; Palefsky, J. M.; Doudna, J. A. CRISPR-Cas12a target binding

unleashes indiscriminate single-stranded DNase activity. *Science* **2018**, *360*, 436−439.
(30) Li, S.-Y.; Cheng, Q.-X.; Wang, J.-M.; Li, X.-Y.; Zhang, Z.-L.; Gao, S.; Cao, R.-B.; Zhao, G.-P.; Wang, J. CRISPR-Cas12a-assisted nucleic acid detection. *Cell Discovery* **2018**, *4*, 1−4.
(31) Broughton, J. P.; Deng, X.; Yu, G.; Fasching, C. L.; Servellita, V.; Singh, J.; Miao, X.; Streithorst, J. A.; Granados, A.; Sotomayor-Gonzalez, A.; et al. CRISPR−Cas12-based detection of SARS-CoV-2. *Nat. Biotechnol.* **2020**, *38*, 870−874.
(32) Zhou, R.; Li, Y.; Dong, T.; Tang, Y.; Li, F. A sequence-specific plasmonic loop-mediated isothermal amplification assay with orthogonal color readouts enabled by CRISPR Cas12a. *Chem. Commun.* **2020**, *56*, 3536−3538.
(33) Liang, M.; Li, Z.; Wang, W.; Liu, J.; Liu, L.; Zhu, G.; Karthik, L.; Wang, M.; Wang, K.-F.; Wang, Z.; Yu, J.; Shuai, Y.; Yu, J.; Zhang, L.; Yang, Z.; Li, C.; Zhang, Q.; Shi, T.; Zhou, L.; Xie, F.; Dai, H.; Liu, X.; Zhang, J.; Liu, G.; Zhuo, Y.; Zhang, B.; Liu, C.; Li, S.; Xia, X.; Tong, Y.; Liu, Y.; Alterovitz, G.; Tan, G.-Y.; Zhang, L.-X. A CRISPR-Cas12a-derived biosensing platform for the highly sensitive detection of diverse small molecules. *Nat. Commun.* **2019**, *10*, 3672.
(34) Xu, Y.; Huo, B.; Li, C.; Peng, Y.; Tian, S.; Fan, L.; Bai, J.; Ning, B.; Gao, Z. Ultrasensitive detection of staphylococcal enterotoxin B in foodstuff through dual signal amplification by bio-barcode and real-time PCR. *Food Chem.* **2019**, *283*, 338−344.
(35) Mandal, S.; Das, P. Ultrasensitive visual detection of mycotoxin citrinin with yellow-light emitting carbon dot and Congo red. *Food Chem.* **2020**, *312*, 126076.
(36) EFSA Panel on Contaminants in the Food Chain (CONTAM). Scientific Opinion on the risks for public and animal health related to the presence of citrinin in food and feed. *EFSA Journal* **2012**, *10*, 2605.
(37) Huo, Y.; Qi, L.; Lv, X.-J.; Lai, T.; Zhang, J.; Zhang, Z.-Q. A sensitive aptasensor for colorimetric detection of adenosine triphosphate based on the protective effect of ATP-aptamer complexes on unmodified gold nanoparticles. *Biosens. Bioelectron.* **2016**, *78*, 315−320.
(38) Liu, M.; Jia, C.; Huang, Y.; Lou, X.; Yao, S.; Jin, Q.; Zhao, J.; Xiang, J. Highly sensitive protein detection using enzyme-labeled gold nanoparticle probes. *Analyst* **2010**, *135*, 327−331.
(39) Atar, N.; Yola, M. L.; Eren, T. Sensitive determination of citrinin based on molecular imprinted electrochemical sensor. *Appl. Surf. Sci.* **2016**, *362*, 315−322.
(40) Sadi, B. S.; Bayat, M.; Tajik, P.; Hashemi, S. J. Citrinin detection by intensified fluorescence signal of a FRET-based immunosensor using magnetic/silica core−shell. *Saudi J. Biol. Sci.* **2018**, *25*, 171−177.
(41) Ji, X.; Xu, J.; Wang, X.; Qi, P.; Wei, W.; Chen, X.; Li, R.; Zhou, Y. Citrinin determination in red fermented rice products by optimized extraction method coupled to liquid chromatography tandem mass spectrometry (LC-MS/MS). *J. Food Sci.* **2015**, *80*, T1438−T1444.
(42) Akyıldırım, O.; Kardaş, F.; Beytur, M.; Yüksek, H.; Atar, N.; Yola, M. L. Palladium nanoparticles functionalized graphene quantum dots with molecularly imprinted polymer for electrochemical analysis of citrinin. *J. Mol. Liq.* **2017**, *243*, 677−681.
(43) Nigović, B.; Sertić, M.; Mornar, A. Simultaneous determination of lovastatin and citrinin in red yeast rice supplements by micellar electrokinetic capillary chromatography. *Food Chem.* **2013**, *138*, 531−538.
(44) Sun, M.; Li, S.; Xu, J.; Zhou, Y.; Fu, R. Simple and accurate spectrofluorimetric method for detecting citrinin in red fermented rice. *Anal. Lett.* **2020**, *53*, 1446−1454.
(45) Wu, S.-W.; Yu, Y.-A.; Liu, B.-H.; Yu, F.-Y. Development of a sensitive enzyme-linked immunosorbent assay and rapid gold nanoparticle immunochromatographic strip for detecting citrinin in monascus fermented food. *Toxins* **2018**, *10*, 354.
(46) Lee, T. P.; Saad, B.; Nakajima, L.; Kobayashi, T. Preparation and characterization of hybrid molecularly imprinted polymer membranes for the determination of citrinin in rice. *Sains Malays.* **2019**, *48*, 1661−1670.

https://doi.org/10.1021/acsfoodscitech.1c00321
ACS Food Sci. Technol. XXXX, XXX, XXX−XXX